Journal of Online Engineering Education
ISSN: 2158-9658 Volume: 17 Issue: 2
Article Received: 15 March 2026 **Revised**: 20 May 2026 **Accepted**: 12 June 2026

Yolo- Smart Fabriscan for Fabric Defect Detection for Improving Missed Detections of Visually Similar Defects

Mrs. C Kavitha[1], Dr. T Ranganayaki[2]
[1]Research Scholar, Department of Computer Science, Eode Arts and Science College Erode
Assistant Professor and Head Department of Computer Science with Data Analytics
St. Joseph's College for Women, Tirupur
ckavitha16183@gmail.com
[2]Research Supervisor, Associate Professor Department of Computer Science, Erode Arts and Science College
Erode
ranganayakitcs.t@gmail.com

Abstract: Fabric defect detection remains a significant challenge, necessitating innovative approaches to enhance detection efficiency and accuracy. The accuracy of fabric detection is better achieved by YOLO based models compared to other Deep Learning (DL) models. However, some categories remain challenging, such as holes and drops defects. Due to the similarities in colour and texture features of these defects, the model tends to misclassify these defects. In addition to that combined with external environmental factors such as changes in lighting conditions, can increase the visual similarity between these two defects, thereby impacting the model's classification accuracy. To improve the typical YOLOv8 models for defect detection classification, customized SPP variations and attention is proposed in this paper to differentiate between fine-grained characteristics. Spatial Pyramid Pooling with Multi-scale Attention and Local Aggregation Network (SPP-MALAN) is proposed. Multi-scale Attention in SPP can improve automatically adjusts the weight distribution in the feature maps to focus more on key areas of the image. This is particularly effective in accurately identifying similar defects in various scales under complex environments like changes in lighting conditions. Local Aggregation Network improves the model's representational capacity by efficiently integrating features from different layers of SPP. Convolution, Batch Normalization and SwiGLU (CBSG) replaces CBS to understand context and identify complex similarities between defects. It provides greater expressivity, leading to better accuracy and convergence of learning model. The proposed model is named as YOLO- Smart FabriScan. Experimental results demonstrate that the proposed YOLO-Smart FabriScan model achieves superior accuracy of 97.01%, 97.06%, and 98.1% on the TILDA 400, AITEX, and Fabric Stain datasets, outperforming all compared models.

Keywords: Fabric Defect Detection, YOLOv8, SPPF, Deep Learning, Multi-scale Attention

1. INTRODUCTION

Textiles are extensively used in clothing, home furnishings, and industrial applications. It not only serves as a key indicator of industry development but also as a fundamental component of cultural, economic, and social progress [1]. In textile industry, the production of fabrics is usually produced with weaving and knitting machines. However, their production process is highly susceptible to variations in raw materials, equipment, and technology, leading to defects such as warp and weft misalignment, holes, and stains [2]. These defects compromise both aesthetic appeal and durability, ultimately diminishing product quality, causing economic losses for enterprises, and negatively impacting consumer experiences.

Hence, fabric defect detection methods are crucial in ensuring proper quality of the fabric [3]. Traditional model relied on manual inspection which are inherently constrained by operator fatigue, inconsistencies in skill levels, and inefficiency, that makes them unsuitable for high-speed manufacturing environments [4]. Therefore, there is a need for automated fabric defect detection for improving fabric quality.

Recent advancements in artificial intelligence (AI) demonstrated effectiveness in identifying simple defects in fabric using advanced learning techniques [5]. It can be divided into Machine Learning (ML) and Deep Learning (DL). ML methods introduced greater flexibility and improved accuracy. ML models analyse different fabrics

Journal of Online Engineering Education
ISSN: 2158-9658 Volume: 17 Issue: 2
Article Received: 15 March 2026 **Revised**: 20 May 2026 **Accepted**: 12 June 2026

using data driven methods to identify patterns and abnormalities in fabric. Even in the cases where minor flaws in fabric occur, these models can detect deviations from conventional fabric patterns [6]. These advancements have enabled ML models to detect even the smallest defects with high precision. For example, Support Vector Machines (SVMs) combined with texture features enhanced defect detection [7]. But these models required labour-intensive feature engineering and struggled with variations in defect types.

The emergence of Deep Learning (DL) models marked a significant breakthrough in fabric defect detection by enabling automatic extraction of features that substantially enhanced accuracy and generalizability [8, 9]. Convolutional Neural Networks (CNNs), a subclass of DL models are quite good at recognizing texture and pattern flaws such as holes, misalignments or stains. Many detection models, including Mask R-CNN [10] and Faster R-CNN [11] have satisfactory performance in fabric defect detection.

Apart from these DL approaches, object detection models have shown remarkable potential in revolutionizing quality control processes in textile manufacturing [12]. Specifically, the YOLO family of models has emerged as a leading framework for real-time object detection. YOLO's single-stage detection framework is highly advantageous for the textile industry, where high-speed production lines necessitate efficient and scalable defect detection systems [13]. YOLO-based systems provide consistent defect detection performance across shifts and varying production volumes, thereby eliminating human error and ensuring scalability in high-throughput environments [14, 15]. The YOLO family of models has emerged as a leading real-time object detection framework, offering a highly efficient and scalable solution for fabric defect detection in high-speed manufacturing environments [16].

Mao et al. [17] presented an enhanced YOLOv8-based framework that integrated attention mechanisms and advanced architectural modules to improve detection accuracy and robustness. The framework incorporates the SimAM attention mechanism within the Spatial Pyramid Pooling Fast (SPPF) module. However, conventional SPPF approximates larger receptive fields using repeated pooling operations, which may lead to limited diversity in multi-scale features and reduced ability to capture fine-grained variations. Additionally, SPPF does not include any mechanism for feature aggregation across layers or attention-based refinement, which are important for handling complex textures.

To overcome these limitations, this research develops a YOLOv8-based YOLO-Smart FabriScan model. In this model, SPPF is replaced with Spatial Pyramid Pooling with Multi-scale Attention and Local Aggregation Network (SPP-MALAN), where SPP extracts multi-scale features using different pooling operations, and MALAN enhances them using ELAN for feature aggregation and EMA for attention-based refinement, improving feature representation and focus on important regions. In YOLOv8-based fabric defect detection, this improvement is significant as fabric images contain repetitive patterns and subtle defects that are difficult to distinguish from normal textures. The SPP module extracts defects at multiple scales, including small yarn irregularities and larger distortions, while MALAN enhances these features using aggregation and attention mechanisms. This enables the YOLOv8 model to better identify and localize both fine and complex defects with improved accuracy and robustness.

2. LITERATURE SURVEY

Liu et al. [18] suggested a PRC-Light YOLO model for fabric defect detection which integrated Partial Convolution (PConv) and Receptive Field Block (RFB) with Content-Aware ReAssembly of FEatures (CARAFE) lightweight upsampling operator. To decrease the computational burden and memory access of the network, a HardSwish activation function is employed with Wise-IOU v3 as bounding box loss function. However, the dataset employed for this model suffers from limitations such as a uniform background, limited quantity and insufficient diversity in defect types.

Lu et al. [19] suggested an enhanced YOLO-BGS model to improve fabric defect detection. The model incorporated a Bi-directional Feature Pyramid Network (BiFPN) to achieve effective multi-scale feature fusion. Additionally, a Shuffle Attention (SA) module was introduced to refine feature classification by enhancing

Journal of Online Engineering Education
ISSN: 2158-9658 Volume: 17 Issue: 2
Article Received: 15 March 2026 **Revised**: 20 May 2026 **Accepted**: 12 June 2026

channel and spatial interactions, while the Global Attention Mechanism (GAM) was employed to improve global contextual understanding and detection accuracy. However, the increased architectural complexity due to multiple attention mechanisms may lead to higher computational overhead.

Ma et al. [20] developed a lightweight fabric defect detection algorithm based on an improved YOLOv8n called GSL-YOLOv8n. To reduce model complexity and parameter count, the study incorporates the GhostNet by designing a C2fGhost module, which replaces standard convolutions with Ghost convolutions. Additionally, a SimAM attention mechanism is integrated at the end of the backbone to suppress redundant background information and enhance feature representation. However, the efficiency gains outweigh significant performance enhancement in more complex or diverse defect scenarios.

Song et al. [21] devised a DA-YOLOv8s model for textile defect detection. The model integrated Deformable Convolutional Networks into the backbone network to enhance feature extraction capability and adopted a Polarized Self-Attention mechanism to strengthen feature fusion across spatial and channel dimensions. Additionally, a Small Object Detection Head (SOHead) was introduced to improve the detection of small-scale defects. However, the approach may still face challenges in handling highly complex backgrounds and extreme variations in defect appearance.

Sun et al. [22] developed an improved YOLOv8n-based model for seamless fabric defect detection. The model introduced a modified SPPF module to enhance multi-scale feature extraction and improve feature fusion. Additionally, the CARAFE upsampling method is employed to adaptively learn pixel relationships, reducing information loss and improving feature map reconstruction for capturing complex textures and subtle defects. However, the model's validation is primarily limited to a specific seamless fabric dataset, which may restrict its generalization capability in diverse real-world textile environments.

Zhou et al. [23] introduced an improved DCFE-YOLOv8n model for fabric defect detection. First, Dynamic Snake Convolution (DSConv) is integrated into the backbone network to extract defect features with elongated and weak defect regions. Then, a Channel Priority Convolutional Attention (CPCA) mechanism layer is added after the SPPF layer to boost the convolutional operations' ability to capture spatial relationships. However, the model struggled with poor generalizability, which reduces it performance.

3. PROPOSED METHODOLOGY

This section describes the proposed model in detail. Figure 1 shows the block diagram of the proposed model.

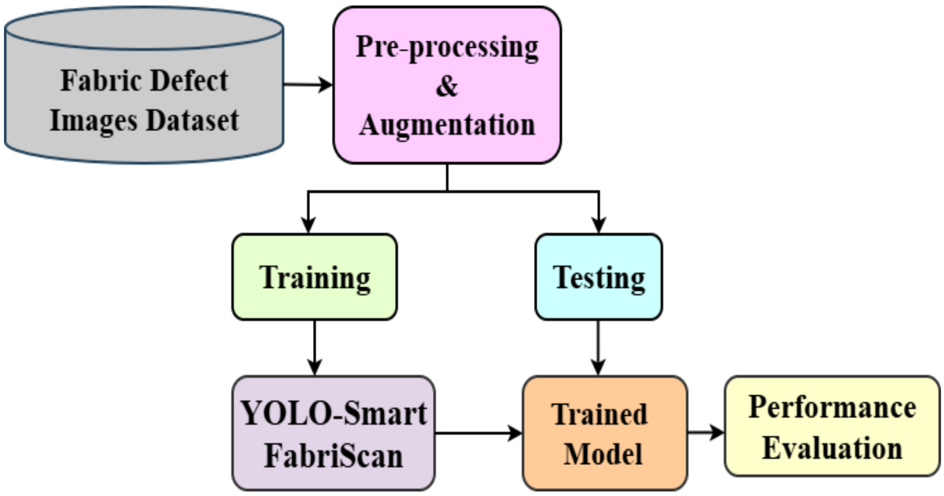

Figure 1. Pipeline of the proposed model

Journal of Online Engineering Education
ISSN: 2158-9658 Volume: 17 Issue: 2
Article Received: 15 March 2026 **Revised**: 20 May 2026 **Accepted**: 12 June 2026

3.1 Image Acquisition and Pre-processing

The images used for this research is collected from various open-source fabric defect images dataset that are available online. Since these images are derived from various databases, pre-processing should be done to mitigate the issues of bias and poor quality. Therefore, the images are first normalized using min-max normalization to transform pixels into a pre-defined range. Next, data augmentation techniques like rotation, scaling, flipping and cropping are applied to expand the size of the dataset.

3.2 YOLOv8- Smart FabriScan Model

YOLOv8, as one of the latest iterations in the YOLO series, is renowned for its efficiency in real-time object detection, combining fast inference speed with high accuracy. Its flexible and modular design allows it to adapt to a wide range of tasks, making it a leading choice for real-time detection applications. To meet varying computational and performance requirements, YOLOv8 is available in multiple versions, each tailored for specific use cases. The backbone network in YOLOv8 is responsible for extracting features from the input image. This process involves five downsampling operations and four feature-extraction modules, resulting in feature maps at four distinct scales: P2, P3, P4, and P5. Each scale corresponds to progressively reduced resolutions, obtained through 2×, 4×, 8×, and 16× downsampling, respectively. These feature maps are subsequently passed into the feature-fusion network, where they are integrated to form a unified representation. The final merged output is delivered to the detection head for object recognition. Key components of the backbone network include:

1. **CBS Module:** The CBS block is composed of a Convolution layer (Conv), batch normalization (BN), and the SiLU activation function, and is responsible for basic feature transformation. However, SiLU limits the model's ability to capture richer contextual and complex feature interactions. To address this limitation, the proposed Convolution, Batch Normalization, and SwiGLU (CBSG) block replaces the conventional CBS structure. SwiGLU improves upon SiLU by incorporating a gating linear unit (GLU). This improves the overall model's capacity to learn complex patterns.
2. **C2f Module:** An enhanced CSPNet-based bottleneck structure with two convolutional layers. It features two branches: one with a convolution layer and multiple bottlenecks, and another with a single convolution module. These branches are merged to retain residual features and enhance feature reuse.
3. **Spatial Pyramid Pooling—Fast (SPPF):** Positioned between the backbone and the feature-fusion network, this module aggregates features from different receptive fields using small pooling layers, effectively enriching feature representation while reducing computational overhead. The structure of the SPPF module is shown in Figure 2. Its main structural process is as follows:

a. First, the number of channels in the input feature map is compressed to half of the original through a 1 × 1 convolution layer, followed by three consecutive max-pooling operations, each performed on the output of the previous pooling layer.

b. Finally, the original compressed features and the results of the three max-pooling operations are concatenated along the channel dimension, and the number of channels is restored to the input channel number through another 1 × 1 convolution.

However, SPPF has certain limitations, as it approximates larger receptive fields using repeated pooling operations, which may lead to limited diversity in multi-scale features and reduced ability to capture fine-grained variations. Additionally, SPPF does not include any mechanism for feature aggregation across layers or attention-based refinement, which are important for handling complex textures. Therefore, in this research, the conventional SPPF is replaced by a novel SPP-MALAN. In this model, SPP extracts multi-scale features using different pooling operations, and MALAN enhances them using LAN for feature aggregation and MA for attention-based refinement, improving feature representation and focus on important regions.

Journal of Online Engineering Education
ISSN: 2158-9658 Volume: 17 Issue: 2
Article Received: 15 March 2026 **Revised**: 20 May 2026 **Accepted**: 12 June 2026

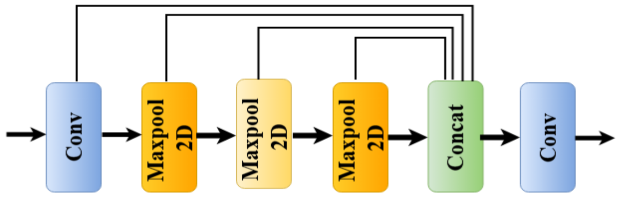

Figure 2. Conventional SPPF module in YOLOv8

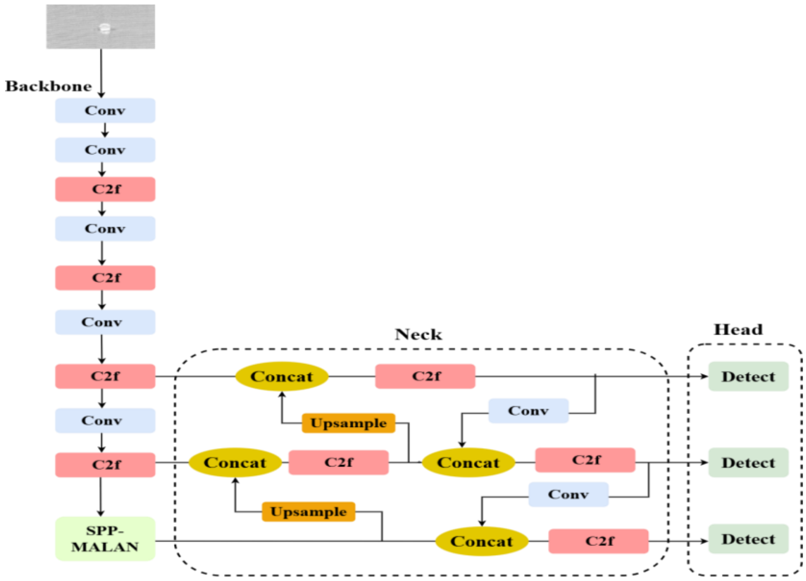

Figure 3. Structure of proposed YOLOv8

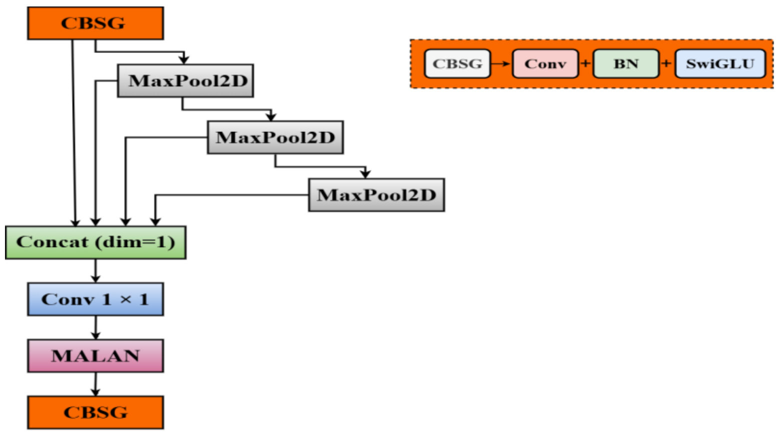

Figure 4. Structure of SPP-MALAN

SPPF replaces SPP by using sequential pooling, which reduces complexity while maintaining comparable receptive field coverage. This design improves efficiency and expressivity, enabling effective capture of both local and global contextual information with faster convergence.

Let the input feature be defined as $X \in R^{B\times C\times H\times W}$. Initially, the input feature passes through the CBSG block, producing a refined feature map while preserving spatial resolution as $X_1 \in R^{B\times C\times H\times W}$. The feature map is then processed using sequential MaxPool2D operations with fixed kernel size, stride = 1, and appropriate padding, ensuring that spatial dimensions remain unchanged. The feature map is then processed using multiple MaxPool2D

Journal of Online Engineering Education
ISSN: 2158-9658 Volume: 17 Issue: 2
Article Received: 15 March 2026 **Revised**: 20 May 2026 **Accepted**: 12 June 2026

operations with different kernel sizes (e.g., 5×5, 9×9, and 13×13), applied in parallel with stride = 1 and appropriate padding to maintain spatial dimensions:

$$X_2 \in Maxpool_{5\times5}(X_1) \quad (1)$$

$$X_3 \in Maxpool_{7\times7}(X_2) \quad (2)$$

$$X_4 \in Maxpool_{9\times9}Maxpool(X_3) \quad (3)$$

All feature maps maintain identical dimensions as in Eq. (4)

$$X_1, X_2, X_3, X_4 \in R^{B\times C\times H\times W} \quad (4)$$

This sequential pooling effectively simulates multi-scale receptive fields enabling the model to capture both local and global contextual information. The outputs of all pooling stages, along with the original feature map, are concatenated along the channel dimension as in Eq. (5)

$$X_{cat} = Concat(X_1, X_2, X_3, X_4) \in R^{B\times 4C\times H\times W} \quad (5)$$

A 1×1 convolution layer is then applied to fuse these features and reduce channel dimensionality.

Then these fused feature maps are passed into MALAN, which integrates Multi-scale Attention (MA) with Layer Aggregation Network (LAN) to enhance feature learning and improve representation capability.

The module begins by dividing the input feature map into g groups along the channel dimension, allowing the model to process features more efficiently while preserving diversity within each group. Each group (with size c/g) is then passed through the MA block independently.

Within each group, the feature map is processed through three parallel pathways: two directional 1×1 branches and one 3×3 branch. The two 1×1 branches focus on capturing global spatial dependencies along specific directions. One branch performs average pooling along the X-axis, while the other performs average pooling along the Y-axis, effectively encoding long-range dependencies in horizontal and vertical directions separately. These pooled features are then concatenated and passed through a 1×1 convolution, enabling interaction between directional information. After this, sigmoid activations are applied to generate attention weights, which are used to recalibrate the feature responses.

In parallel, the 3×3 branch captures local spatial context. Its output is refined through global average pooling and SoftMax operations to emphasize informative regions. The interaction between branches is established via matrix multiplication, enabling fusion of global directional attention and local spatial features. This produces complementary attention maps that encode both precise positional information and broader contextual dependencies. Finally, the fused features are aggregated and projected separately through a 1×1 convolution to produce the output. Figure 5 shows the structure of MALAN.

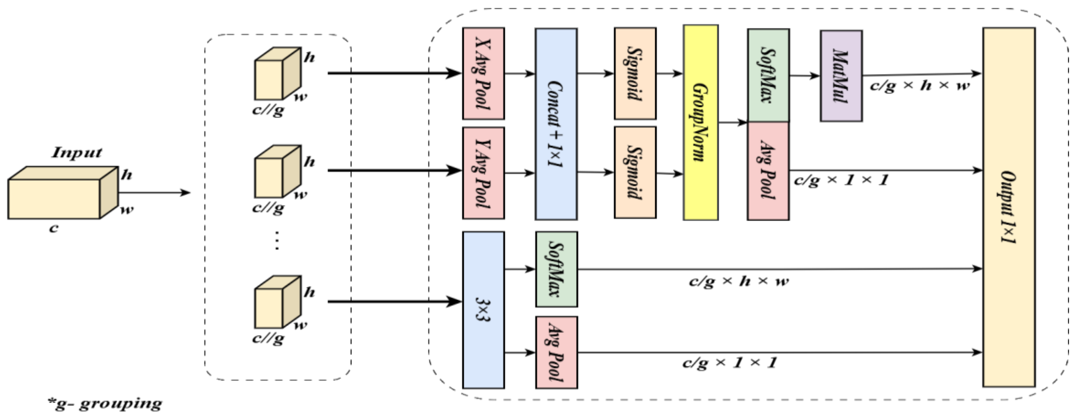

Figure 5. Structure of MALAN

ISSN: 2158-9658 Volume: 17 Issue: 2
Article Received: 15 March 2026 **Revised**: 20 May 2026 **Accepted**: 12 June 2026

Algorithm 1: Proposed YOLO-Smart FabriScan Model

Input: Fabric image datasets

Output: Detected fabric defects with bounding boxes and class labels

1. Normalize input images using min-max normalization
2. Resize images to required input size
3. Apply data augmentation (rotation, flipping, scaling, cropping)
4. Input image I is passed into YOLOv8 backbone
5. Replace conventional SPPF with SPP–MALAN module

Spatial Pyramid Pooling (SPP):

a. Apply CBSG block for initial feature refinement
b. Perform sequential max-pooling with multiple kernel sizes to simulate multi-scale receptive fields.
c. Maintain spatial dimensions using stride = 1 and appropriate padding.
d. Concatenate pooled feature maps with the original feature map along the channel dimension.
e. Apply a 1×1 convolution to fuse features and reduce channel dimensionality.

MALAN module:

6. Split feature maps into g channel groups.
7. For each group:
8. Apply X-axis and Y-axis average pooling to capture directional global context.
9. Concatenate pooled features and pass through a 1×1 convolution.
10. Apply sigmoid activation to generate directional attention weights.
11. In parallel, apply a 3×3 convolution to extract local spatial features.
12. Use global average pooling + softmax to emphasize important regions.
13. Perform matrix multiplication (MatMul) to fuse global and local features.
14. Concatenate outputs from all branches to expand channel representation.
15. Apply a 1×1 convolution to fuse features and reduce dimensionality.
16. Pass refined features through the CBSG block for further enhancement.
17. Upsample high-level features.
18. Generate multi-scale feature maps
19. Feed each feature map into detection heads to predict bounding boxes and class probabilities
20. Output the final detected fabric defects

4. RESULTS AND DISCUSSION

This section evaluates the efficiency of the proposed YOLO-Smart FabriScan Model by comparing it with standard models. Table 1 shows the parameter settings for the proposed and existing models.

Table 1. Parameters Settings

Parameters	**Specifications**
FCN, U-Net, DeepLabv3	
Image size	256×256
Number of epochs	50
Batch size	16
Weight decay	0.0005
Deep Labv3, Mask R-CNN	
Backbone	ResNet50, ResNet101
Epochs	100
Mask R-CNN	
Batch size	4
Image size	512×512
Confidence threshold	0.5
YOLOV8n, YOLOv5, YOLOv10, YOLOv11, U-Net, YOLO-FabriScan, Proposed YOLO-Smart FabriScan	
Batch Size	32
Momentum	0.937
Image size	640×640
Epochs	100
Optimizer	Adam
Epochs	100
IoU threshold	0.5
Learning Rate	0.001
Confidence threshold	0.25
YOLO-FabriScan, YOLO- Smart FabriScan	
Backbone	CSPDarknet
Image size	640×640
Weight Decay	0.0005
Loss	Cross Entropy

4.1 Dataset Description

This research employs three datasets:

1. **TILDA 400 dataset [24]:** This dataset consists of 25,636 images collected for defect analysis, including five classes: good, hole, objects, oil spot, and thread error. Among these, the good class contains 23,170 defect-free images, while the remaining 2,466 images belong to different defect categories. The distribution of samples across classes is highly uneven, with defect classes having significantly fewer instances compared to the defect-free class, leading to a severe class imbalance. To address this issue, data augmentation techniques such as rotation, flipping, scaling, and brightness adjustment were applied, particularly to the minority defect classes. After augmentation, each class was normalized to approximately 5,000 samples, resulting in a balanced dataset of around 25,000 images, ensuring equal representation of all classes for effective model training.

2. **AITEX Fabric Image database [25]:** This dataset consists of 246 images collected from 7 different fabric types. Among these, 140 images are defect-free, with 20 samples for each fabric type. In addition, the dataset includes 106 defective images, which contain various types of fabric defects. These defective samples are

Journal of Online Engineering Education
ISSN: 2158-9658 Volume: 17 Issue: 2
Article Received: 15 March 2026 **Revised**: 20 May 2026 **Accepted**: 12 June 2026

unevenly distributed across different fabric types, leading to class imbalance. Therefore, data augmentation techniques such as rotation, flipping, scaling, and brightness adjustment were applied to this dataset. After augmentation, the dataset was expanded to 520 images, with 240 defect images and 280 non-defect images.

3. **Fabric Stain dataset [26]:** This dataset consists of 466 images collected for fabric stain detection, comprising two classes: stain and no defect. Among these, the no defect class contains 398 images, while the stain class includes 68 images. The dataset exhibits class imbalance, with a significantly higher number of non-defective samples compared to defective ones. To mitigate this imbalance, data augmentation techniques were applied, primarily to the minority class (stain). Additionally, controlled sampling was performed to maintain a balanced distribution between the two classes. After preprocessing, the stain class was increased to approximately 250 samples, and the no defect class was adjusted to around 275 samples, resulting in a balanced dataset of about 525 images, ensuring improved learning and generalization during model training.

To prepare the dataset for model training, the images were divided into 80% for training and 20% for testing. The split details for each classes of every datasets are given in tables 2,3 and 4.

Table 2. Split details of TILDA 400 dataset

Classes	**Before augmentation**			**After augmentation**		
	Training	**Testing**	**Total**	**Training**	**Testing**	**Total**
Good	18536	4634	23170	4160	1040	5200
Hole	270	67	337	3840	960	4800
Objects	698	175	873	4092	1023	5115
Oil spot	509	127	636	4016	1004	5020
Thread error	496	124	620	4000	1000	5000
Total	20509	5127	25636	20108	5027	25135

Table 3. Split details of AITEX Fabric Image Database

Classes	**Before augmentation**			**After augmentation**		
	Training	**Testing**	**Total**	**Training**	**Testing**	**Total**
Defect	85	21	106	192	48	240
No defect	112	28	140	224	56	280
Total	197	49	246	416	104	520

Table 4. Split details of Fabric Stain Dataset

Classes	**Before augmentation**			**After augmentation**		
	Training	**Testing**	**Total**	**Training**	**Testing**	**Total**
Stain	54	14	68	200	50	250
No defect	318	80	398	220	55	275
Total	372	94	466	420	105	525

Journal of Online Engineering Education
ISSN: 2158-9658 Volume: 17 Issue: 2
Article Received: 15 March 2026 **Revised**: 20 May 2026 **Accepted**: 12 June 2026

4.2 Evaluation metrics

The performance measures used to evaluate the proposed model is defined as follows:

4.2.1 Segmentation Metrics:

i) **Dice Coefficient:** The Dice Coefficient is calculated by doubling the area of overlap between the predicted segmentation and the ground truth, then dividing by the total number of pixels in both segmentations.

$$Dice = \frac{2TP}{2TP+FP+FN} \tag{17}$$

ii) **Intersection over Union (IoU):** It measures the overlap between the predicted segmentation and the ground truth.

$$IoU = \frac{TP}{TP+FP+FN} \tag{18}$$

iii) **Hausdorff Distance:** It measures the maximum distance between boundary points of two segmented shapes, acting as a sensitivity metric for boundary mismatches in segmentation.

$$H(A,B) = max\ (\|a-b\| \tag{19}$$

4.2.2 Classification Metrics:

Let TP denotes the True Positives, FP represents the False Positives, TN represents True Negatives and FN represents False Negatives.

i) **Accuracy:** It measures the overall correctness of predictions.

$$Accuracy = \frac{TP+TN}{TP+TN+FP+FN} \tag{20}$$

ii) **Precision:** It evaluates how many predicted defects are actually correct.

$$Precision = \frac{TP}{TP+FP} \tag{21}$$

iii) **Recall:** It measures how many actual defects are correctly detected.

$$Recall = \frac{TP}{TP+FN} \tag{22}$$

iv) **F1-Score:** It is the harmonic mean of precision and recall.

$$F1-score = \frac{2\times Precision\times Recall}{Precision+Recall} \tag{23}$$

v) **mAP 50:** It evaluates object detection performance at an Intersection over Union (IoU) threshold of 0.5.

$$mAP50 = \frac{1}{N}\sum_{i=1}^{N} AP_i \tag{24}$$

vi) **mAP 50-95:**

$$mAP_{50-95} = \frac{1}{10}\sum_{i=0}^{9} mAP_{IoU_i} \tag{25}$$

vii) **ROC-AUC (Receiver Operating Characteristic - Area Under Curve):** It measures performance across all threshold levels by plotting the TP Rate vs. FP Rate with AUC indicating how well the model separates positive from negative classes.

4.3 Performance Evaluation

The confusion matrices for both the datasets are given in Figures 7-9.

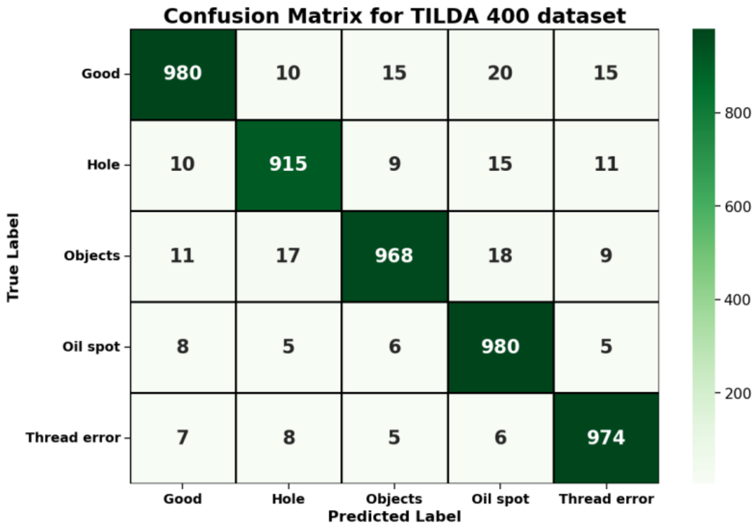

Figure 7. Confusion matrix of proposed model in TILDA 400 dataset

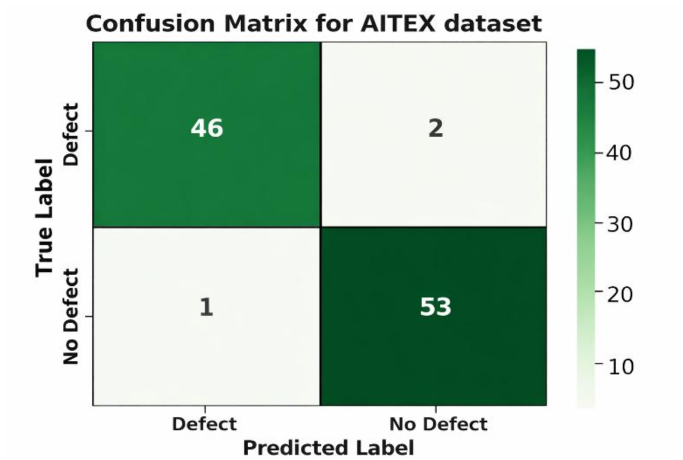

Figure 8. Confusion matrix of proposed model in AITEX Fabric Image dataset

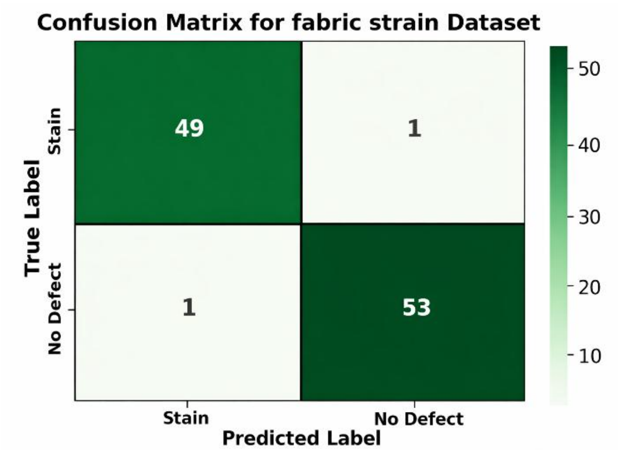

Figure 9. Confusion matrix of proposed model in Fabric Stain dataset

Journal of Online Engineering Education
ISSN: 2158-9658 Volume: 17 Issue: 2
Article Received: 15 March 2026 **Revised**: 20 May 2026 **Accepted**: 12 June 2026

4.3.1 Segmentation Evaluation

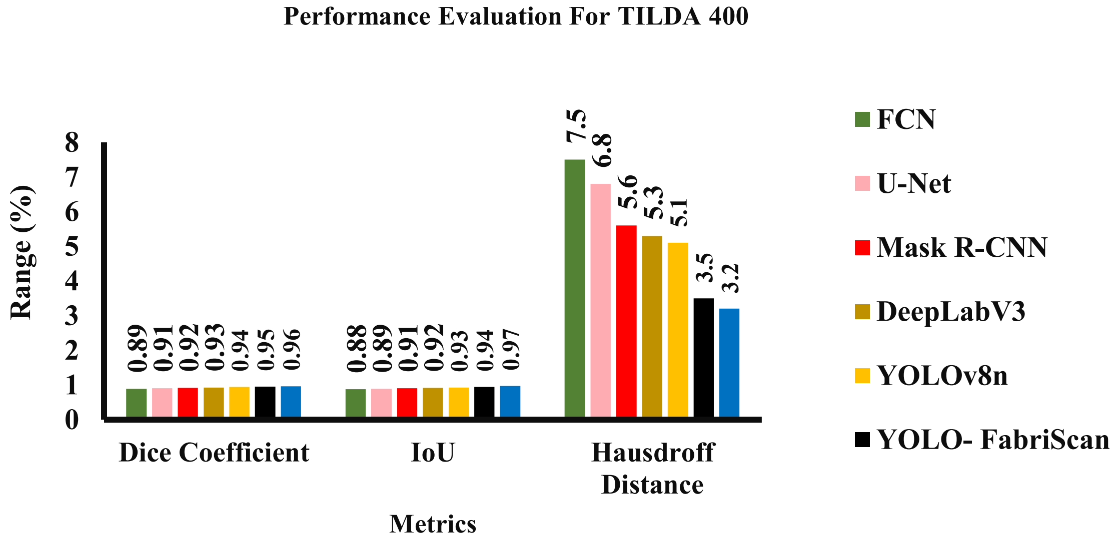

Figure 10. Comparison of proposed YOLO-Smart FabriScan and existing segmentation models on TILDA 400 dataset

Figure 10 presents the performance comparison of different deep learning models on the TILDA 400 dataset using Dice Coefficient, IoU, and HD metrics. The proposed YOLO-Smart FabriScan model demonstrates superior segmentation performance across all evaluation metrics. In terms of Dice Coefficient, the proposed model achieves 0.96, showing an improvement of approximately 7.87%, 5.49%, 4.35%, 3.23%, 2.13%, and 1.05% over the compared models. For IoU, YOLO-Smart FabriScan attains 0.97, outperforming the baseline models by approximately 10.23%, 8.99%, 6.59%, 5.43%, 4.30%, and 3.19%, respectively. For HD, the proposed model achieves the lowest value of 3.2, indicating a reduction of approximately 57.33%, 52.94%, 42.86%, 39.62%, 37.25%, and 8.57% compared to the other models, respectively.

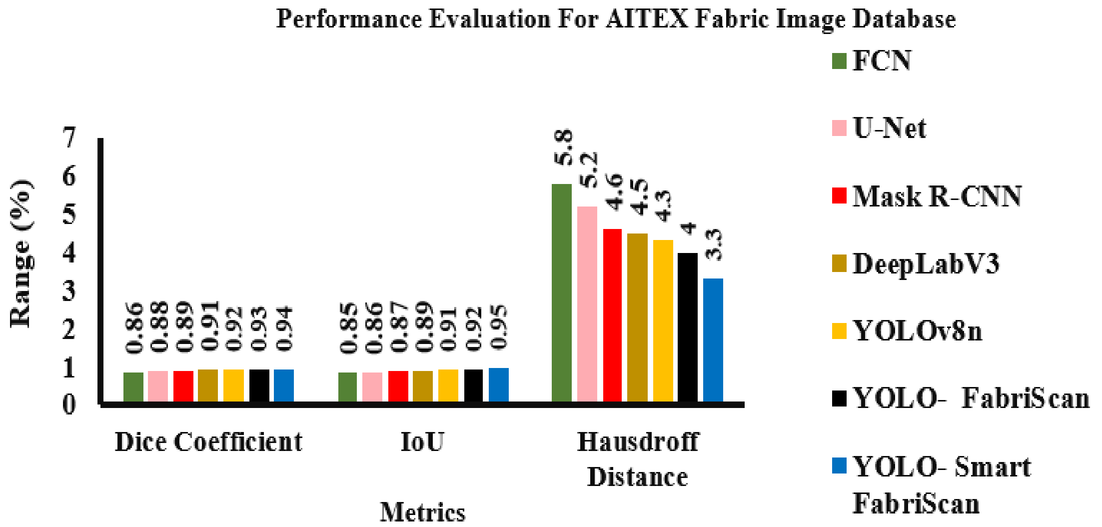

Figure 11. Comparison of proposed YOLO-Smart FabriScan and existing segmentation models on AITEX Fabric Image Dataset

Figure 11 presents the performance comparison of different deep learning models on the AITEX Fabric Image Database using Dice Coefficient, IoU, and HD metrics. The proposed YOLO- Smart FabriScan model demonstrates superior segmentation performance across all evaluation metrics. In terms of Dice Coefficient, the proposed model achieves 0.94, showing an improvement of approximately 9.30%, 6.82%, 5.62%, 3.30%, 2.17%, and 1.08% over the compared models. For IoU, YOLO-Smart FabriScan attains 0.95, outperforming the baseline models by approximately 11.76%, 10.47%, 9.20%, 6.74%, 4.40%, and 3.26%, respectively. For HD, the proposed model achieves the lowest value of 3.3, indicating a reduction of approximately 43.10%, 36.54%, 28.26%, 26.67%, 23.26%, and 17.50% compared to the other models, respectively.

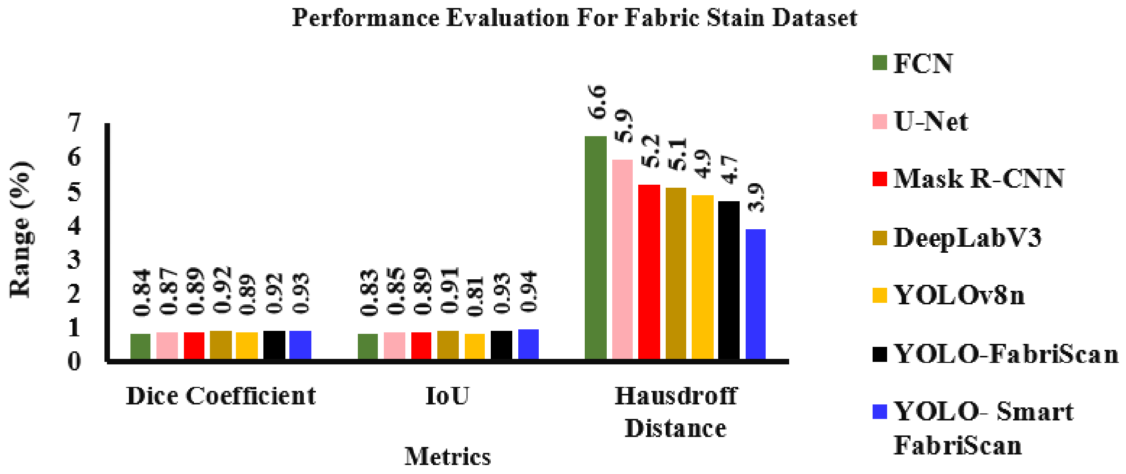

Figure 12. Comparison of proposed YOLO- Smart FabriScan and existing segmentation models on Fabric Stain dataset

Figure 12 presents the performance comparison of different deep learning models on the Fabric Stain Dataset using Dice Coefficient, IoU, and HD metrics. The proposed YOLO-Smart FabriScan model demonstrates superior segmentation performance across all evaluation metrics. In terms of Dice Coefficient, the proposed model achieves 0.93, showing an improvement of approximately 10.71%, 6.90%, 4.49%, 1.09%, 4.49%, and 1.09% over the compared models. For IoU, YOLO-Smart FabriScan attains 0.94, outperforming the baseline models by approximately 13.25%, 10.59%, 5.62%, 3.30%, 16.05%, and 1.08%, respectively. For HD, the proposed model achieves the lowest value of 3.9, indicating a reduction of approximately 40.91%, 33.90%, 25.00%, 23.53%, 20.41%, and 17.02% compared to the other models, respectively.

4.3.2 Classification Evaluation

Figure 13 presents the performance comparison of different YOLO-based models on the TILDA 400 dataset using Accuracy, Precision, Recall, F1-Score, mAP50, and mAP50–95 metrics. The proposed YOLO-Smart FabriScan model demonstrates superior detection performance across all evaluation metrics. The proposed model achieves an Accuracy of 97.01%, with improvements of approximately 13.82%, 10.11%, 6.72%, 3.48%, 2.12%, and 0.69% over the compared models. Precision reaches 97.34%, showing gains of about 9.73%, 6.11%, 3.67%, 2.49%, 2.36%, and 1.04%, respectively. For Recall, YOLO-Smart FabriScan attains 97.06%, improving performance by approximately 8.95%, 6.97%, 3.52%, 2.78%, 2.16%, and 1.03%. The F1-Score further increases to 97.21%, with enhancements of around 7.69%, 4.74%, 2.81%, 1.87%, 1.84%, and 0.80% compared to the baseline models. In addition, the proposed model achieves 96.55% in mAP50 and 96.78% in mAP50–95, outperforming the other models by approximately 5.79%, 3.52%, 2.26%, 1.27%, 1.04%, and 0.54% and 9.82%, 6.31%, 3.51%, 2.70%, 2.06%, and 1.03%, respectively.

Journal of Online Engineering Education
ISSN: 2158-9658 Volume: 17 Issue: 2
Article Received: 15 March 2026 **Revised**: 20 May 2026 **Accepted**: 12 June 2026

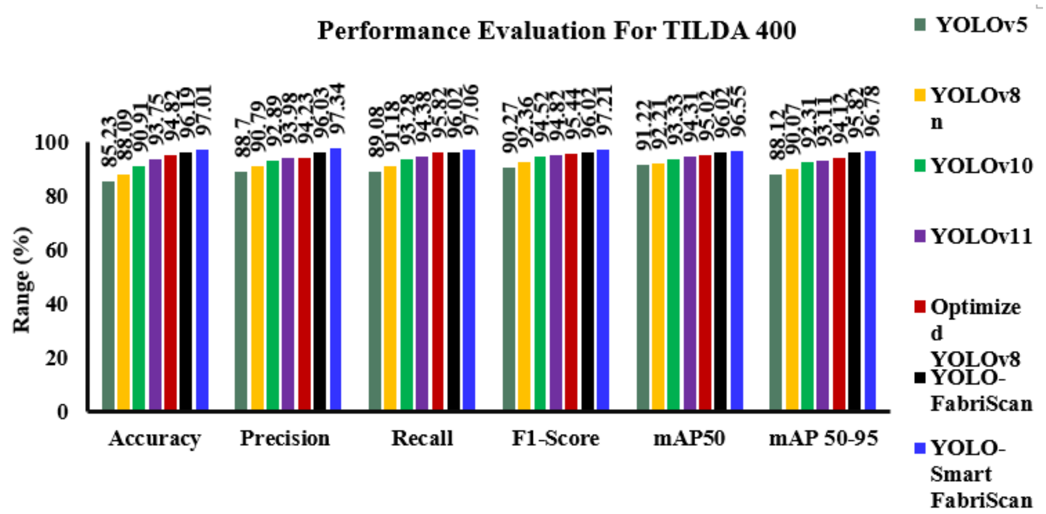

Figure 13. Comparison of proposed YOLO-Smart FabriScan and standard classification models on TILDA 400 dataset

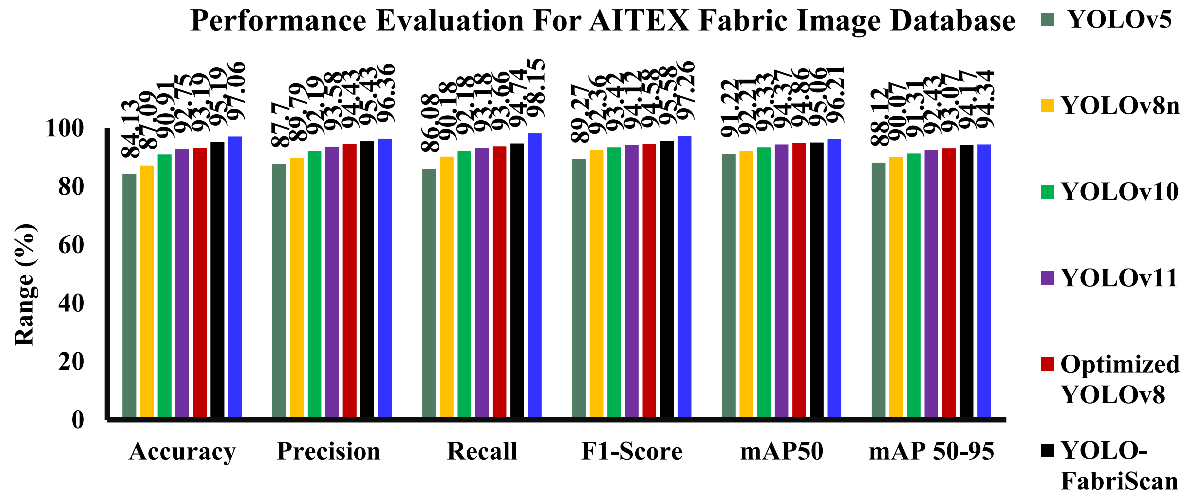

Figure 14. Comparison of proposed YOLO-Smart FabriScan and standard classification models on AITEX Fabric Image Dataset

Figure 14 presents the performance comparison of different YOLO-based models on the AITEX Fabric Image Database using accuracy, precision, recall, f1-score, mAP50, and mAP50–95 metrics. The proposed YOLO-Smart FabriScan model demonstrates superior and consistent detection performance across all evaluation metrics. The proposed model achieves an Accuracy of 97.06%, with improvements of approximately 15.36%, 11.45%, 6.76%, 4.63%, 4.15%, and 1.97% over the compared models. Precision reaches 96.36%, showing gains of about 9.87%, 7.07%, 4.17%, 2.98%, 1.93%, and 1.07%, respectively. For Recall, YOLO-Smart FabriScan attains 98.15%, improving performance by approximately 14.00%, 10.82%, 6.48%, 5.33%, 4.79%, and 2.78%. The F1-Score further increases to 97.26%, with enhancements of around 8.96%, 5.14%, 2.88%, 1.96%, 1.91%, and 1.15% compared to the baseline models. In addition, the proposed model achieves 96.21% in mAP50 and 94.34% in mAP50–95, outperforming the other models by approximately 5.47%, 3.08%, 1.84%, 1.48%, 1.35%, and 0.63% and 6.22%, 3.69%, 2.17%, 1.91%, 1.36%, and 0.18%, respectively.

Article Received: 15 March 2026 **Revised**: 20 May 2026 **Accepted**: 12 June 2026

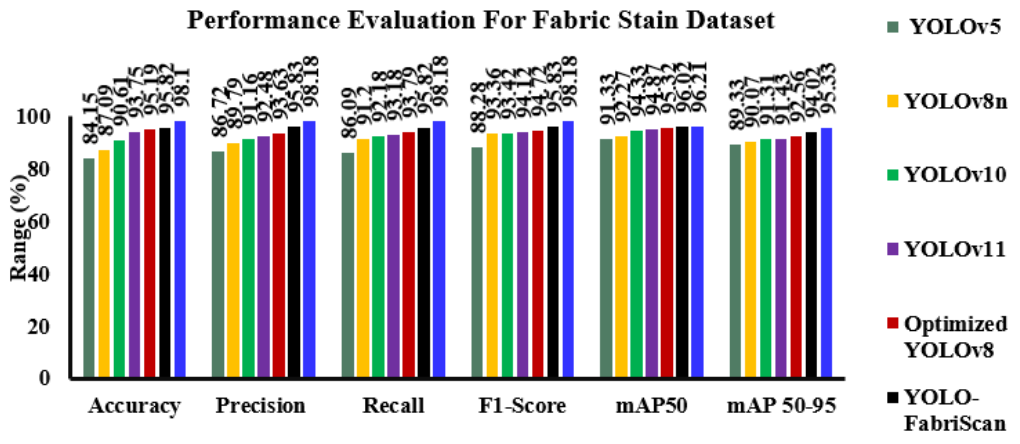

Figure 15. Comparison of proposed YOLO-FabriScan and standard classification models on Fabric Stain Dataset

Figure 15 presents the performance comparison of different YOLO-based models on the Fabric Stain Dataset using accuracy, precision, recall, f1-score, mAP50, and mAP50–95 metrics. The proposed YOLO-Smart FabriScan model demonstrates superior and consistent detection performance across all evaluation metrics. The proposed model achieves an accuracy of 98.1%, with improvements of approximately 16.47%, 12.64%, 7.40%, 4.55%, 2.95%, and 1.24% over the compared models. Precision reaches 98.18%, showing gains of about 13.22%, 10.13%, 6.84%, 4.07%, 3.67%, and 2.43%, respectively. For Recall, YOLO-Smart FabriScan attains 98.18%, improving performance by approximately 14.09%, 11.28%, 6.50%, 5.17%, 4.67%, and 2.95%. The F1-Score further increases to 98.18%, with enhancements of around 11.29%, 5.88%, 4.25%, 3.22%, 3.07%, and 2.04% compared to the baseline models. In addition, the proposed model achieves 96.21% in mAP50 and 95.33% in mAP50–95, outperforming the other models by approximately 5.35%, 3.27%, 1.98%, 1.51%, 0.93%, and 0.20% and 6.80%, 4.39%, 3.39%, 2.75%, 2.77%, and 1.39%, respectively.

4.3.3 ROC Comparison

Figure 16 presents the ROC curve comparison of different YOLO-based models on the TILDA 400 dataset. The proposed YOLO-Smart FabriScan model demonstrates superior classification capability, achieving the highest Area Under the Curve (AUC) value. The proposed model attains an AUC of 0.96, showing an improvement of approximately 45.45%, 37.14%, 31.51%, 24.68%, 15.66%, and 3.23% over the compared models.

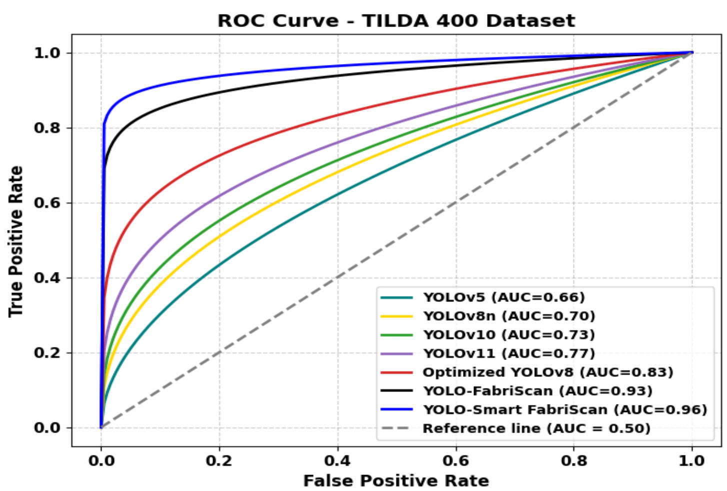

Figure 16. ROC Comparison of proposed and standard classification models on TILDA 400 dataset

Journal of Online Engineering Education
ISSN: 2158-9658 Volume: 17 Issue: 2
Article Received: 15 March 2026 **Revised**: 20 May 2026 **Accepted**: 12 June 2026

Figure 17 presents the ROC curve comparison of different YOLO-based models on the AITEX Fabric Image Database. The proposed YOLO-Smart FabriScan model demonstrates superior classification performance, achieving the highest Area Under the Curve (AUC) among all models. The proposed model attains an AUC of 0.95, showing an improvement of approximately 66.67%, 53.23%, 46.15%, 37.68%, 15.85%, and 4.40% over the compared models.

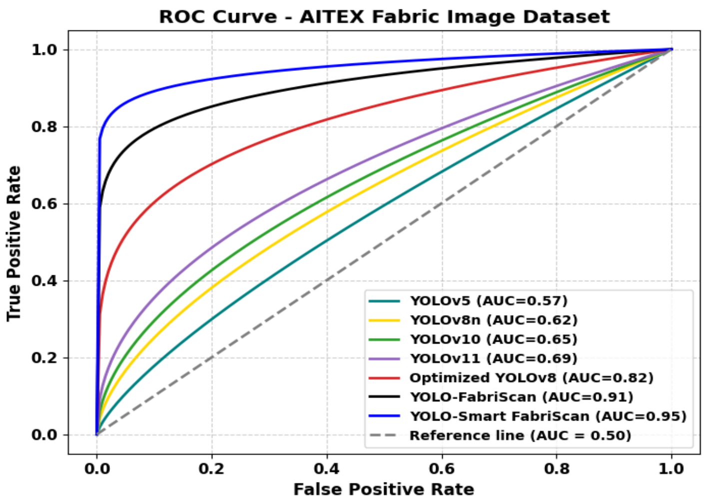

Figure 17. ROC Comparison of proposed and standard classification models on AITEX Fabric Image dataset

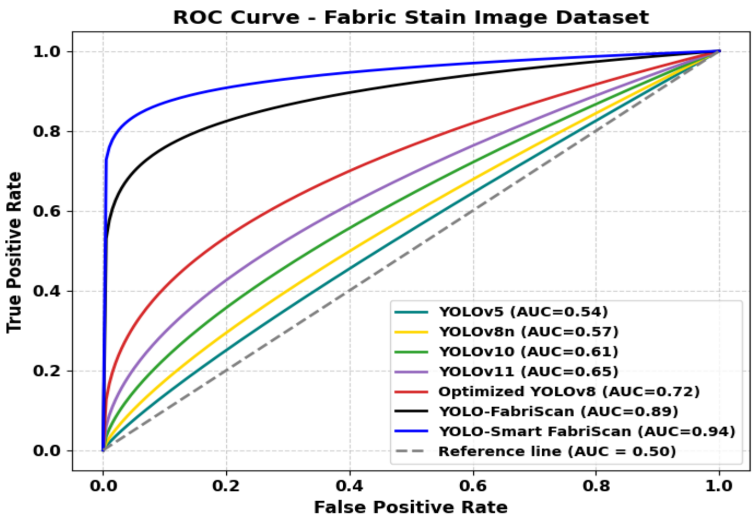

Figure 18. ROC Comparison of proposed and standard classification models on Fabric Stain dataset

Figure 18 presents the ROC curve comparison of different YOLO-based models on the Fabric Stain Dataset. The proposed YOLO-Smart FabriScan model demonstrates superior classification performance, achieving the highest Area Under the Curve (AUC) among all models. The proposed model attains an AUC of 0.94, showing an improvement of approximately 74.07%, 64.91%, 54.10%, 44.62%, 30.56%, and 5.62% over the compared models.

5. CONCLUSION

This paper presents a novel YOLOv8-based YOLO-Smart FabriScan framework to address the challenge of detecting visually similar and fine-grained fabric defects under complex environmental conditions. The proposed model enhances the conventional YOLOv8 architecture by replacing the standard SPPF module with the SPP–

MALAN module. The SPP component improves multi-scale feature extraction by capturing both local and global contextual information, while the MALAN module, consisting of Multi-scale Attention and Layer Aggregation Network, effectively refines feature representation through attention-driven enhancement and multi-level feature aggregation. Additionally, the integration of the CBSG block improves non-linear feature learning and strengthens the model's ability to distinguish subtle defect variations. The performance of the proposed model is validated on three benchmark datasets, namely TILDA 400, AITEX Fabric Image Database, and Fabric Stain Dataset. Experimental results demonstrate that the proposed YOLO-Smart FabriScan model achieves superior accuracy of 97.01%, 97.06%, and 98.1% on the TILDA 400, AITEX, and Fabric Stain datasets, respectively, outperforming all compared models.

REFERENCES

[1] Kabish, A. K. (2023). Textile and clothing production and trading-the way to industrial economy development. Ethiopian Journal of Science and Technology, 16(Special), 1-12.

[2] Kuo, C. F. J., Wang, W. R., & Barman, J. (2022). Automated optical inspection for defect identification and classification in actual woven fabric production lines. Sensors, 22(19), 7246.

[3] Liu, J., Wang, C., Su, H., Du, B., & Tao, D. (2019). Multistage GAN for fabric defect detection. IEEE Transactions on Image Processing, 29, 3388-3400.

[4] Alibin, R. (2025). Mastering Efficiency and Quality: A Qualitative Study On Techniques and Practices in Garment Mass Production. Asian Research Journal of Education, 2(4), 22-31.

[5] Machado, R., Barros, L. A., Vieira, V., Silva, F. D. D., Costa, H., & Carvalho, V. (2025). Textile defect detection using artificial intelligence and computer vision—a preliminary deep learning approach. Electronics, 14(18), 3692.

[6] Ribeiro, R., Pilastri, A., Moura, C., Morgado, J., & Cortez, P. (2023). A data-driven intelligent decision support system that combines predictive and prescriptive analytics for the design of new textile fabrics. Neural Computing and Applications, 35(23), 17375-17395.

[7] Huang, Y., Yi, M., Yang, W., & Yang, M. (2022, February). Research on surface defect intelligent detection technology of non-woven fabric based on support vector machine. In 2022 IEEE international conference on electrical engineering, big data and algorithms (EEBDA) (pp. 895-898). IEEE.

[8] Liu, Q., Wang, C., Li, Y., Gao, M., & Li, J. (2022). A fabric defect detection method based on deep learning. IEEE access, 10, 4284-4296.

[9] Beljadid, A., Tannouche, A., & Balouki, A. (2022). Automatic fabric defect detection employing deep learning. International Journal of Electrical and Computer Engineering, 12(4), 4129.

[10] Moganam, P. K., & Sathia Seelan, D. A. (2022). Deep learning and machine learning neural network approaches for multi class leather texture defect classification and segmentation. Journal of Leather Science and Engineering, 4(1), 7.

[11] Revathy, G., & Kalaivani, R. (2024). Fabric defect detection and classification via deep learning-based improved Mask RCNN. Signal, Image and Video Processing, 18(3), 2183-2193.

[12] Chen, M., Yu, L., Zhi, C., Sun, R., Zhu, S., Gao, Z., ... & Zhang, Y. (2022). Improved faster R-CNN for fabric defect detection based on Gabor filter with Genetic Algorithm optimization. Computers in Industry, 134, 103551.

[13] Kaur, R., & Singh, S. (2023). A comprehensive review of object detection with deep learning. Digital Signal Processing, 132, 103812.

[14] Liu, C., Tao, Y., Liang, J., Li, K., & Chen, Y. (2018, December). Object detection based on YOLO network. In 2018 IEEE 4th information technology and mechatronics engineering conference (ITOEC) (pp. 799-803). IEEE.

[15] Zhao, Z. Q., Zheng, P., Xu, S. T., & Wu, X. (2019). Object detection with deep learning: A review. IEEE transactions on neural networks and learning systems, 30(11), 3212-3232.

[16] Ali, M. L., & Zhang, Z. (2024). The YOLO framework: A comprehensive review of evolution, applications, and benchmarks in object detection. Computers, 13(12), 336.

[17] Mao, Y., Wang, G., Ma, Y., & Gui, X. (2025). Enhancing Fabric Defect Detection With Attention Mechanisms and Optimized YOLOv8 Framework. IEEE Access.

[18] Liu, B., Wang, H., Cao, Z., Wang, Y., Tao, L., Yang, J., & Zhang, K. (2024). PRC-Light YOLO: An efficient lightweight model for fabric defect detection. Applied Sciences, 14(2), 938.

[19] Lu, G., Xiong, T., & Wu, G. (2024). YOLO-BGS optimizes textile production processes: enhancing YOLOv8n with bi-directional feature pyramid network and global and shuffle attention mechanisms for efficient fabric defect detection. Sustainability, 16(18), 7922.

[20] Ma, S., Liu, Y., & Zhang, Y. (2024). Fabric defect detection based on improved lightweight YOLOv8n. Applied Sciences, 14(17), 8000.

[21] Song, W., Lang, D., Zhang, J., Zheng, M., & Li, X. (2025). Textile defect detection algorithm based on the improved yolov8. IEEE Access, 13, 11217-11231.

[22] Sun, Q., Noche, B., Xie, Z., & Huang, B. (2025). Research on seamless fabric defect detection based on improved YOLOv8n. Applied Sciences, 15(5), 2728.

[23] Zhou, L., Ma, B., Dong, Y., Yin, Z., & Lu, F. (2025). DCFE-YOLO: A novel fabric defect detection method. PloS one, 20(1), e0314525.

[24] https://www.kaggle.com/datasets/angelolmg/tilda-400-64x64-patches

[25] https://www.kaggle.com/datasets/nexuswho/aitex-fabric-image-database

[26] https://www.kaggle.com/datasets/priemshpathirana/fabric-stain-dataset